Medium Voltage DC Power Systems on Ships: an Off-line Parameter Estimation for Tuning the Controllers' Linearizing Function

D. Bosich, *Member, IEEE*, G. Sulligoi, *Senior Member, IEEE*, E. Mocanu, Student *Member, IEEE* and M. Gibescu, *Member, IEEE*

***Abstract*--Future shipboard power systems using Medium Voltage Direct (MVDC) technology will be based on a widespread use of power converters for interfacing generating systems and loads with the main DC bus. Such a heavy exploitation makes the voltage control challenging in the presence of tightly controlled converters. By modeling the latter as Constant Power Loads (CPLs), one possibility to ensure the bus voltage stability is offered by the Linearizing via State Feedback technique (LSF), whose aim is to regulate the generating DC-DC power converters to compensate for the destabilizing effect of the CPLs. Although this method has been shown to be effective when system parameters are perfectly known, only a partial linearization can be ensured in case of parameter mismatch, thus jeopardizing the system stability. In order to improve the linearization, therefore guaranteeing the voltage stability, an estimation method is proposed in this paper. To this aim, off-line tests are performed to provide the input data for the estimation of model parameters. Such estimated values are subsequently used for correctly tuning the linearizing function of the DC-DC converters. Simulation results for bus voltage transients show that in this way converters become sources of stabilizing power.**

***Index Terms* -- Constant Power Load, DC-DC power converters, Linearization via State Feedback, model reduction, parameter estimation, Heuristic Optimization.**

I. Introduction

NOWADAYS power converters are the key technology for innovative shipboard power system designs [1]. If the Integrated Power System (IPS) constituted the cornerstone in the past [2], important drivers (e.g. improved control of power flows, enhanced system efficiency, fuel savings, reduction of power system volume, modularity in ship design) are pushing the research toward the new concept of Integrated Electric and Electronic Power System (IEEPS) [3], where a widespread presence of power converters is anticipated. In this context, the Medium Voltage Direct Current (MVDC) distribution represents a promising technology for contributing to the aforementioned drivers, as proposed in [4]-[7]. In such a system, the lead role is given to power converters aimed at interfacing the AC generation side with the AC (or DC) load side: on one hand, this pervasive presence gives the possibility to reach the IEEPS targets [3], on the other hand, it opens relevant challenges with regards to DC voltage stability. This may be jeopardized by the well-known Constant Power Load (CPL) destabilizing effect [8]-[9].

Such a voltage instability is given by the simultaneous presence of high-bandwidth controlled load-side converters (leading to CPL behavior), and RLC filtering stages, aimed at guaranteeing the power quality requirements [4]. One possibility to overcome the instability is the voltage actuator approach, where power converters on the generation side are properly controlled to behave as sources of stabilizing powers [9]. A different possibility for solving the system instability may be given by the load converter approach, where the CPL control bandwidth is conveniently reduced for preventing the destabilizing effect [9]. Focusing on the voltage actuator approach, several control strategies may be exploited [10], among others Active Damping (AD) [11]-[12] and Linearization via State Feedback (LSF) [13]-[14]. In the specific area of LSF control, this paper proposes to overcome a typical limit of this technique, i.e. partial linearization in the presence of parameter mismatch.

The LSF technique is a powerful solution to guarantee the voltage stability of risky DC shipboard power systems, where a relevant CPL power is supplied through critical RLC filtering stages (i.e. with negative damping factor) on the generation side [14]. Keeping in mind that the instability is given by the presence of nonlinear loads (CPLs), the LSF technique is aimed at cancelling the destabilizing effect of these loads by properly controlling the action of generating DC converters. In the presence of perfect knowledge about system parameters and nonlinear feedback signals, the LSF can be properly tuned to compensate for the effect of CPLs. In such a case, thanks to a nonlinear, linearizing function perfectly calibrated on the system, it is possible to establish an input-output linear relationship governing the power system dynamics. Subsequently, a control function may be used for performing the desired pole placement, as widely discussed in [14]. Whereas errors on the signal measurements (i.e. negative or positive offsets with consequent under/over-linearization effects) can be avoided by installing accurate probes, different strategies must be conceived for facing the inaccurate

D. Bosich and G. Sulligoi are with the Department of Engineering and Architecture, University of Trieste, 34127 Trieste, Italy, (e-mail: dbosich@units.it; gsulligoi@units.it).

E. Mocanu and M. Gibescu are with the Department of Electrical Engineering, Eindhoven University of Technology, 5600 MB Eindhoven, The Netherlands, (e-mail: e.mocanu@tue.nl; m.gibescu@tue.nl).

parameter settings. As a matter of fact, in the presence of a parameter mismatch, the linearization is only partial, and when insufficient may lead to system instability [14]. Although the over-linearization [13] can be a strategy to solve instability even in the presence of parameter mismatch, possible saturation of the highly stressed power converters [15] is a disadvantage, thus motivating the investigation of an alternative approach in this work.

In this regard, one possibility to safeguard against the inaccurate linearization is offered by the off-line parameter estimation. Once a snapshot (voltage transient) of the system is obtained, deterministic and stochastic methods [16] may be exploited for calibrating the parameters of a reduced system model in order to obtain a convergence among the reference voltage transient and the model output. In the presence of a perfect convergence between the two transients, the estimated parameters are an exact replica of the real ones. In this case, the LSF technique may be consequently tuned to successfully linearize the DC power system. As a main theoretical contribution, we introduce a novel parameter estimation procedure, named Selective Search (SS). Its capabilities are validated by comparison with a more commonly used method, i.e. Particle Swarm Optimization (PSO).

In the following, the paper organization is explained. Section II describes the MVDC power system topology, together with the detailed configuration of a single DC generating system, the multiconverter simplified circuit model and the related reduced model. The latter is capable of summarizing the equivalent filter parameters (installed versus designed) of two power system configurations. The effect of parameter mismatch is investigated in section III, where a large-signal voltage stability is used for showing the shrinking of RAS (i.e. Region of Asymptotic Stability) in the presence of partial linearizations. Section IV defines the off-line tests used for obtaining the reference signals and the estimation algorithms. The performance of the proposed estimation in preserving the linearizing functionality is evaluated in section V, while section VI concludes the paper.

II. MVDC Shipboard Power System

In this section, a multiconverter MVDC power system controlled by the LSF technique [14] is presented. This sets the context for the estimation procedure of the parameters of the reduced system model. The estimation procedure proposed in this paper is therefore aimed at determining the system parameters for correctly applying the LSF control strategy envisaged in [14].

In subsection I-A, the topology is described together with the DC generating system data, whereas in subsection I-B particular attention is spent on the filtering stages. Subsection I-C proposes a convenient model reduction for studying the bus voltage transients in the presence of LSF, while the power system configurations are treated in subsection I-D. The latter is important for clarifying the off-line tests to be performed for obtaining the reduced model in the scenarios given by a sudden generator disconnection.

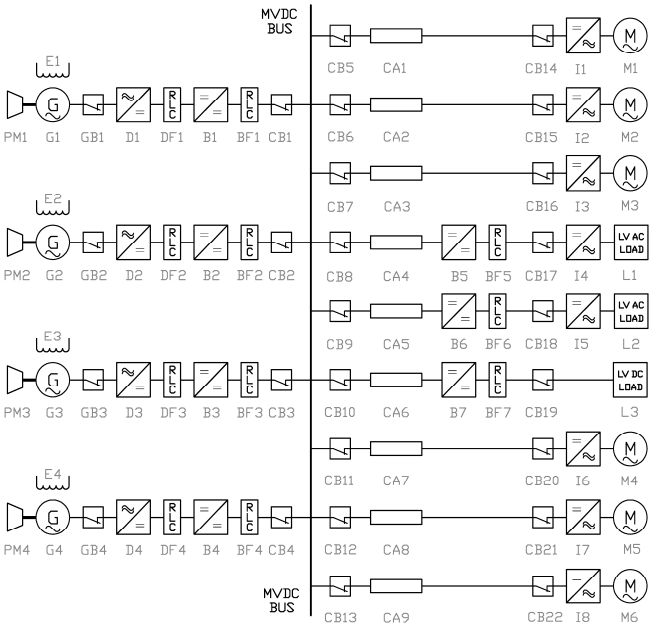

Figure 1. Multiconverter MVDC power system [14].

A. Power System Topology

The MVDC shipboard power system used in this paper (Fig. 1) has been already discussed in [14]. In this system, the bus voltage V_0 is equal to 6000 V (this value is compliant with the IEEE recommendations [4]), while the total generating power P_t is 52.5 MW. The interface role between the AC generators and the DC bus is played by the cascade of diode bridge rectifiers (D1-D4) and buck converters (B1-B4). This solution (Fig. 2) is exploited for three important reasons [9]: 1) the buck converters' capability to perfectly decouple the generators from the DC bus control; 2) the use of buck converters does not cause reactive power impact on the AC source; 3) the high switching frequencies (usually in the order of kHz) of DC-DC power converters will guarantee notable dynamics performance on the DC bus voltage control. Focusing on filtering arrangements, the four RLC stages (BF1-BF4) are capable of ensuring the power quality requirements [4], but at the same time they are responsible for the voltage destabilizing effect [8]-[9] in the presence of the nine tightly controlled power converters (I1-I3, B5-B7, I6-I8). The latter are modeled as nonlinear CPLs (i.e. $I_L=P/V$), although a recent dissertation [17] has demonstrated that this ideal modeling is not the worst-case condition from a control standpoint. Anyhow, the filters' parameter estimation introduced in this work is independent of CPL modeling, and is applicable even when this ideal representation is replaced by a more realistic one. An overview of the DC generating system k (k=1,2,…4) is provided in Fig. 2 and Table I, where the following parameters (n states for rated value) are defined:

- U_{nk}: AC machine rated line-to-line output voltage
- V_{dnk}: rated voltage on rectifier filter capacitor
- V_{nk}: rated voltage on buck filter capacitor
- P_{nk}: buck converter rated output power
- D_{nk}: buck converter rated duty cycle
- I_{nk}: rated current in buck filter inductor
- f_{sk}: buck converter switching frequency

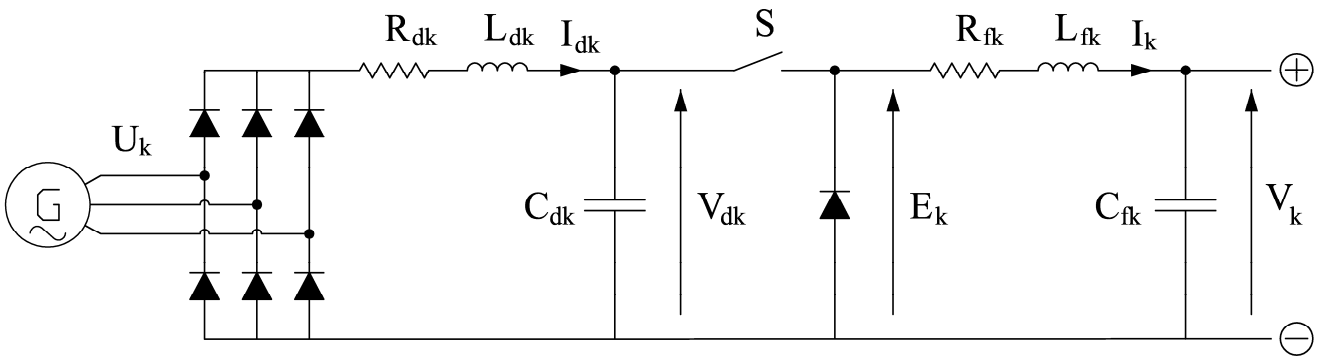

Figure 2. DC generating system (AC synchronous machine + filtered diode bridge rectifier + filtered buck converter).

TABLE I. DC generating systems parameters [14].

	BF1/BF3	BF2/BF4
U_{nk} [V]	6600	6600
V_{dnk} [V]	8910	8910
V_{nk} [V]	6000	6000
P_{nk} [MW]	15.75	10.50
D_{nk}	0.67	0.67
I_{nk} [A]	2494	1662
f_{sk} [Hz]	1500	1500

TABLE II. Designed filters parameters [14].

	BF1/BF3	BF2/BF4
R_{fk} [mΩ]	126.63	189.95
L_{fk} [mH]	1.75	2.62
C_{fk} [μF]	346.35	230.90

TABLE III. Ratio among filter parameters: installed vs. designed.

	BF1	BF2	BF3	BF4
R_{fk}^*/R_{fk}	0.83	1.18	0.88	0.79
L_{fk}^*/L_{fk}	1.03	0.93	0.96	0.87
C_{fk}^*/C_{fk}	0.71	0.75	0.79	0.81

The DC generating system k is shown in Fig. 2, where filtered diode bridge rectifier is cascaded with filtered buck converter (S represents the static switch). In such a figure, the two DC poles (connected to the bus) are depicted on the right, whereas AC excitation system and circuit breakers are not shown for the sake of simplicity. Focusing on Table I, it is remarkable to notice the low values of rated duty cycles chosen during the design process (i.e. D_{nk} = 0.67). Such values allow sufficient duty cycle margins (i.e. 1-0.67 = 0.33) for avoiding buck converters' saturation [15] during the transients given by ordinary (e.g. load connections) or extraordinary perturbations (e.g. faults, generating system disconnections).

B. MVDC Simplified Circuit Model

As envisaged in [14], the nine shipboard loads (Fig. 1) may be aggregated in an equivalent CPL (i.e. P_{eq}), whereas the cables (CA1-CA9) may be neglected due to the short distances onboard. In this way, the simplified circuit of Fig. 3 is used for properly describing the DC voltage dynamics, where E_k is the DC-DC buck converter voltage output as shown in Fig. 2. As in [14], the four RLC filtering stages are designed with the values in Table II, to take into account buck converter losses ($\Delta P_{\%}$=5) and to guarantee proper peak-to-peak voltage ripple

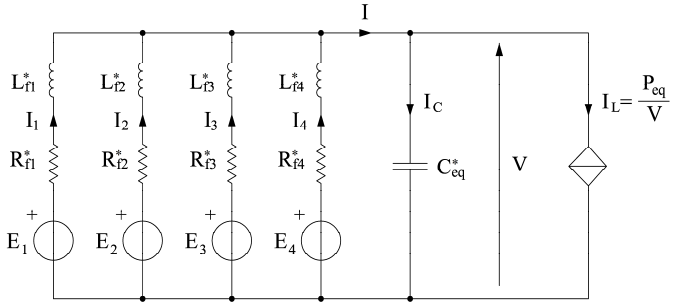

Figure 3. Simplified circuit model of the multiconverter MVDC system [14].

($\Delta V_{\%}$=3) and current ripple ($\Delta I_{\%}$=30) in compliance with the requirements in [4]. Particular attention is spent on the sizing of capacitors: as a matter of fact, system stability is evidently enhanced by the presence of large capacitors [9]-[10], but on the other hand practical issues suggest to limit these components in shipboard applications. Among others, the risk of fire/explosion (i.e. catastrophic failure in shipboard power system [18]) which is strongly dependent on capacitors' size and the peak value of DC short-circuit current, which is directly proportional to the capacitance value [19]. Moreover, large capacitors in Medium Voltage DC applications are expensive (due to high insulation cost) and bulky, thus limiting the expected compactness advantages of MVDC applications with respect to MVAC shipboard power systems [7]. For all these reasons, the presented paper is based on the choice of limited filter capacitances, whose parameters have been already justified in the published paper [14].

Looking at Table III, it is possible to prefigure a discrepancy between the designed filters parameters (R_{fk}, L_{fk}, C_{fk}) and the values characterizing the actually installed components (R_{fk}^*, L_{fk}^*, C_{fk}^*) shown in Fig. 3. Focusing on the components mainly responsible for the CPL voltage instability (i.e. L_{fk}^* and C_{fk}^*), only a slight difference is conceivable for the inductances, which is practically given by the intrinsic tolerance. On the other hand, a large discrepancy (even up to 29% for C_{f1}^*) is presumable for the capacitances. Indeed, such components are subject to electrolytic aging, resulting in a capacitance drop [20]. This aspect is of paramount importance when DC voltage instability is solved by applying LSF technique: since installed capacitors are smaller than the designed ones, an insufficient linearizing effect based on the designed values can be foreseen (see section III for details).

C. Model Reduction: 2nd order LSF controlled model

The voltage stability of the DC power system in the presence of a large CPL may be ensured by the application of the LSF technique [14]. By conveniently regulating the four buck converters' voltage outputs by means of linearizing functions F_k, such a control strategy has the aim of compensating for the nonlinear CPL effect, thus guaranteeing a resultant linear system. To better understand the action of the F_k functions, a convenient model reduction can be conceived. Particularly, by applying Thévenin's theorem at the capacitor's terminals and considering the open-circuit hypothesis (Fig. 3), a reduced model may be obtained as in Fig. 4, where function F is the equivalent linearizing function to be subtracted from the Thévenin equivalent voltage source E_{th}. The equivalent filter parameters (R_{eq}^*, $L_{eq}^*$and C_{eq}^*) are found by computing the parallel equivalent and making the unique pole assumption ($R_{fk}^*/L_{fk}^* \cong R_{eq}^*/L_{eq}^*=1/T_f^*$). Since the typical distance between these real poles is negligible compared to the distance to the complex poles, this hypothesis is verified in practice [14].

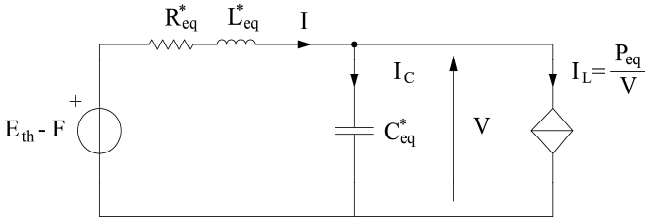

Figure 4. Second-order reduced model.

The reduced-order model is described by two state equations (1). By deriving the first state equation of (1), equation (2) can be found, and then equation (3) is determined by combining (2) and second state equation of (1). By rearranging first equation of (1), equation (4) is defined. Finally, a second-order nonlinear differential equation in the state variable V (DC bus voltage) may be constructed (5) by combining (3) and (4):

$$\begin{cases} \dot{V} = \dfrac{1}{C_{eq}^*}\left(I - \dfrac{P_{eq}}{V}\right) \\ \dot{I} = \dfrac{1}{L_{eq}^*}\left(E_{th} - F - V - R_{eq}^* I\right) \end{cases} \tag{1}$$

$$\ddot{V} = \frac{1}{C_{eq}^*}\left(\dot{I} + \frac{P_{eq}}{V^2}\dot{V}\right) \tag{2}$$

$$\ddot{V} = \frac{1}{L_{eq}^* C_{eq}^*}\left(E_{th} - F - V - R_{eq}^* I\right) + \frac{1}{C_{eq}^*}\frac{P_{eq}}{V^2}\dot{V} \tag{3}$$

$$I = C_{eq}^*\dot{V} + \frac{P_{eq}}{V} \tag{4}$$

$$\ddot{V} + \left(\frac{R_{eq}^*}{L_{eq}^*}\right)\cdot\dot{V} + \left(\frac{1}{L_{eq}^* C_{eq}^*}\right)\cdot V + \Lambda = \frac{1}{L_{eq}^* C_{eq}^*}\left(E_{th} - F\right) \tag{5}$$

where the Λ term (6) groups all the nonlinear terms, while F as defined in (7) is the nonlinear function which pursues the feedback compensation to linearize the state-space model (5).

$$\Lambda = -\left(\frac{1}{C_{eq}^*}\frac{P_{eq}}{V^2}\right)\cdot\dot{V} + \left(\frac{R_{eq}^*}{L_{eq}^* C_{eq}^*}\right)\cdot\frac{P_{eq}}{V} \tag{6}$$

$$\frac{F}{L_{eq}^* C_{eq}^*} = \left(\frac{1}{C_{eq}^c}\frac{P_{eq}}{V^2}\right)\cdot\dot{V} - \left(\frac{R_{eq}^c}{L_{eq}^c C_{eq}^c}\right)\cdot\frac{P_{eq}}{V} \cong -\Lambda \tag{7}$$

Evidently, the complete compensation is achievable only when the nonlinear feedback F is perfectly tuned to the function Λ. That means on one hand the perfect correspondence among control parameters (R_{eq}^c, L_{eq}^c and C_{eq}^c) and the parameters of the installed filters (R_{eq}^*, L_{eq}^* and C_{eq}^*), and on the other one precise knowledge about the time-varying functions (P_{eq}, V, dV/dt). Assuming that the latter are known and available for the definition of F, eq. (5) can be rewritten as (8) to highlight how a parameter mismatch leads to the presence of nonlinear terms, even when LSF control is applied.

$$\begin{aligned} &\ddot{V} + \left(\frac{R_{eq}^*}{L_{eq}^*}\right)\cdot\dot{V} + \left(\frac{1}{L_{eq}^* C_{eq}^*}\right)\cdot V + \left(\frac{1}{C_{eq}^c} - \frac{1}{C_{eq}^*}\right)\frac{P_{eq}}{V^2}\dot{V} + \\ &+ \left(\frac{R_{eq}^*}{L_{eq}^* C_{eq}^*} - \frac{R_{eq}^c}{L_{eq}^c C_{eq}^c}\right)\cdot\frac{P_{eq}}{V} = \frac{E_{th}}{L_{eq}^* C_{eq}^*} \end{aligned} \tag{8}$$

Relationship (8) forms the basis for the Lyapunov theory developed in section III to demonstrate how the Region of Asymptotic Stability (RAS) tends to shrink in the presence of a divergence between control and installed filter parameters.

D. Power system configurations

The last equation (8) describes the voltage dynamics of a MVDC shipboard power system where the linearizing function F only partially compensates for the nonlinear terms, since perfect correspondence with installed parameters is not achievable in practice. Such an equation depends on equivalent filter parameters, which are time-varying as the circuit breakers (CBs) connecting the 4 buck converters and filters (BFs) to the bus may change status. Although the possible configurations are 11 (6 with 2 BFs, 4 with 3 BFs and one with 4 BFs), this paper studies only the effect of parameter mismatch in the presence of a sudden disconnection [14] of generating system 3. For the temporally consecutive scenarios (1 and 2), equivalent filter data are given in Table IV.

TABLE IV. Equivalent filter parameters: installed versus designed.

	SCENARIO 1	SCENARIO 2
CBs	CB_{123} ON CB_4 OFF	CB_{12} ON CB_{34} OFF
R_{eq}^* [mΩ]	43.57	71.55
R_{eq} [mΩ]	47.49	75.98
L_{eq}^* [mH]	0.64	1.03
L_{eq} [mH]	0.65	1.05
C_{eq}^* [μF]	692.71	419.09
C_{eq} [μF]	923.61	577.26
T_f^* [ms]	14.68	14.46
T_f [ms]	13.79	13.79
R_{eq}^*/R_{eq}	0.92	0.94
L_{eq}^*/L_{eq}	0.98	0.99
C_{eq}^*/C_{eq}	0.75	0.73
T_f^*/T_f	1.06	1.05

III. Effect of Parameters Mismatch

The result of the parameter mismatch is the partial compensation of the Λ term, therefore the power system, albeit controlled by LSF, remains nonlinear. This eventuality has been already investigated in [14], where a small-signal analysis demonstrates the criticality of the capacitive component. Particularly, in Scenario 2, a tiny difference (-5%) between the installed capacitance and the designed one used for calculating the *F* function resulted in an insufficient linearization [14], leading to system instability (i.e. negative damping factor).

A. Large-signal voltage stability

Since a shipboard power system is an islanded grid where perturbations may have notable consequences, the parameter mismatch effect on LSF capability must be evaluated not only by means of the small-signal analysis as in our previous work [14], but also by taking into account the effect of large perturbations. In this regard, the Lyapunov theory [21] is a valuable method for studying the large-signal stability of a nonlinear system. Given the parameters of Scenario 2, P_{eq}=18.5 MW, we study perturbations capable of moving the two states (*V* bus voltage and *I* total load current) far from the equilibrium point (V_0 = 6 kV, $I_0 = P_{eq}/V_0$ = 3.1 kA). The study presented hereafter provides the Regions of Asymptotic Stability (RASs), sufficient but not necessary areas in the *V*-*I* plane where the large-signal stability is guaranteed. The determination of the RAS is based on the methodology discussed in [22]. Particularly, to define the Lyapunov function and its first derivative, equation (8) is rearranged using notation (9)-(10), where capacitances and resistances defined by (11) are variable within the range specified by (12):

$$\ddot{V} + h(V)\cdot\dot{V} + g(V) = 0 \quad (9)$$

$$\begin{cases} h(V) = \dfrac{R^*_{eq}}{L^*_{eq}} - \dfrac{P_{eq}}{C_F V^2} \\ g(V) = \dfrac{1}{L^*_{eq} C^*_{eq}}\left[V + R_F \dfrac{P_{eq}}{V} - E_{th}\right] \end{cases} \quad (10)$$

$$\begin{cases} \dfrac{1}{C_F} = \dfrac{1}{C^*_{eq}} - \dfrac{1}{C^c_{eq}} \\ R_F = R^*_{eq} - R^c_{eq}\left(\dfrac{L^*_{eq} C^*_{eq}}{L^c_{eq} C^c_{eq}}\right) \end{cases} \quad (11)$$

$$\begin{cases} 0 < \dfrac{1}{C_F} < \dfrac{1}{C^*_{eq}} \\ 0 < R_F < R^*_{eq} \end{cases} \quad (12)$$

Then, expression (13) is proposed to define the Lyapunov function (14) and its first derivative $d\Psi(V,I)/dt$ (15):

$$\begin{cases} \Psi = \dfrac{1}{2}\left\{\dot{V} + \displaystyle\int_{V_0}^{V} h(\vartheta)d\vartheta\right\}^2 + \int_{V_0}^{V} g(\vartheta)d\vartheta \\ \dot{\Psi} = -g(V)\displaystyle\int_{V_0}^{V} h(\vartheta)d\vartheta \end{cases} \quad (13)$$

$$\Psi(V,I) = \frac{1}{2}\left\{\frac{I}{C^*_{eq}} - \frac{P_{eq}}{C^*_{eq} V} + \frac{R^*_{eq}}{L^*_{eq}}(V - V_0) + \frac{P_{eq}}{C_F V} - \frac{P_{eq}}{C_F V_0}\right\}^2 + \quad (14)$$

$$+ \frac{1}{L^*_{eq} C^*_{eq}}\left\{\frac{V^2 - V_0^2}{2} + R_F P_{eq} \log_e\left|\frac{V}{V_0}\right| - E_{th}(V - V_0)\right\}$$

$$\dot{\Psi}(V,I) = \frac{1}{L^*_{eq} C^*_{eq}}\left[V + R_F \frac{P_{eq}}{V} - E_{th}\right]\cdot\left[-\frac{R^*_{eq}}{L^*_{eq}}(V - V_0) - \frac{P_{eq}}{C_F V} + \frac{P_{eq}}{C_F V_0}\right] \quad (15)$$

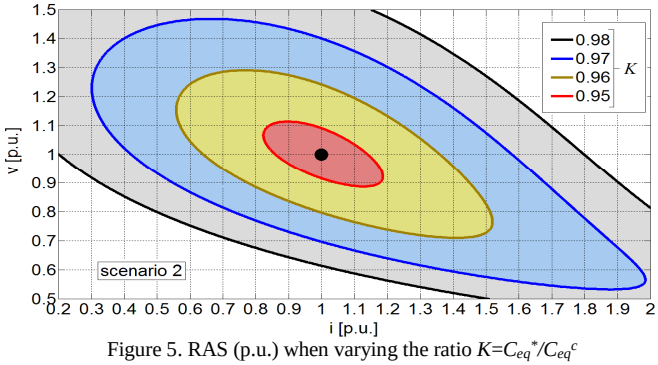

Figure 5. RAS (p.u.) when varying the ratio $K=C_{eq}^*/C_{eq}^c$

As explained in [22], once the two limits V_{min} (16) and I_t (17) are specified, the plane *k* and therefore the RAS can finally be expressed by (18) and (19).

$$\begin{cases} \dot{\Psi}(V) \le 0 \\ V \ge \dfrac{P_{eq}}{V_0 \cdot \left(\dfrac{R^*_{eq} C_F}{L^*_{eq}}\right)} := V_{min} \end{cases} \quad (16)$$

$$\begin{cases} \Omega(I) = \Psi(V_{min}, I) \\ \dfrac{d\Omega(I)}{dI} = 0 \Rightarrow I_t = \dfrac{R^*_{eq} C_F}{L^*_{eq}} V_0 \end{cases} \quad (17)$$

$$k = \Psi(V_{min}, I_t) \quad (18)$$

$$RAS = \{(V,I) : \Psi(V,I) \le k\} \quad (19)$$

Unlike the sensitivity analysis investigated in [14] which is based on the small-signal hypothesis, the proposed nonlinear theory can be used for performing a large-signal analysis, in order to determine the RAS, as depicted in Fig. 5, for various value of the ratio $K = C_{eq}^*/C_{eq}^c$. This shows the shrinking of the stability region in the presence of a mismatch between installed capacitance C_{eq}^* and control capacitance C_{eq}^c (note that other control parameters are assumed equal to the installed ones). By expressing the ratio C_{eq}^*/C_{eq}^c with the term *K*, it is possible to conclude the criticality of the capacitive term. Indeed, a small discrepancy (*K*=0.95) is able to strongly reduce the RAS, thus jeopardizing the bus voltage stability. Even worse results are obtained if C_{eq}^c is put equal to the designed value: a *K* parameter of 0.73 (Table IV) results in an unstable behavior (i.e. empty RAS being $V_{min} > V_0$). Such an issue highlights the need of an estimation (as presented in section IV) for evaluating the control parameters on which to synthesize the function *F*.

IV. Parameter Estimation

The parameter estimation is based on the comparison between a measured voltage transient (A) resulting from the full model, and the output (B) of a reduced model. The reduced model parameters are fit so as to minimize the Root Mean Square Error (RMSE) between system responses A and B. For providing a complete estimation, 11 off-line tests are necessary in order to define the filter parameters in the 11 different configurations. For the sake of simplicity, only two tests are proposed in this paper for realizing the parameter estimation in the scenarios previously presented (Scenario 1 and 2). The method can clearly be applied to a complete estimation capable of correctly tuning the linearizing function in each power system configuration. For starting the estimation procedure, firstly it is necessary to define the tests to be

performed to obtain the measured transients (subsection IV-A). Then, the reduced model for estimation will be detailed in subsection IV-B, whereas the methods for parameter estimation will be discussed from IV-C to IV-F.

A. Off-line tests

The paper is aimed at properly tuning the function F for two hypothetical scenarios, taken as examples (Table IV): initial Scenario 1 (CB_{123} ON, CB_4 OFF), and final Scenario 2 (CB_{12} ON, CB_{34} OFF), which follows a hypothetical generating system disconnection as conceived in [14]. Therefore, two off-line tests are to be planned for estimating the reduced model parameters in the two aforementioned scenarios. In these tests, any influence given by LSF control must be avoided by deactivating the linearizing function F, thus the measured voltage transients (A) can be triggered only by connection of linear loads (i.e. low-bandwidth controlled converters) in order to prevent any destabilizing effect. In other words, only a linear load step P_T is acceptable, since the system is devoid of any kind of stabilizing actions. Particularly, assuming a power system working in no-load condition (t<1 s in Figs. 6 and 7) where buck converter outputs E_k are regulated by constant duty cycles D_k, a voltage transient can be forced by imposing a linear load connection at t=1 s. Once the linear load is connected, the reference voltage transient for the estimation procedure can be measured by a digital oscilloscope, whose sampling frequency should be sufficiently high in order to conveniently register the voltage dynamics (e.g. 100 kHz is selected in the proposed examples, anticipating a certain voltage behavior in terms of natural angular frequency and damping factor). Since the voltage measurements are naturally characterized by a superimposed noisy signal (e.g. standard deviation of about 0.025), a nonlinear bilateral filter (21 samples window, σ_d=3, σ_r=1) is to be employed for obtaining a filtered signal [23]-[24], consequently used as reference for the estimation algorithms.

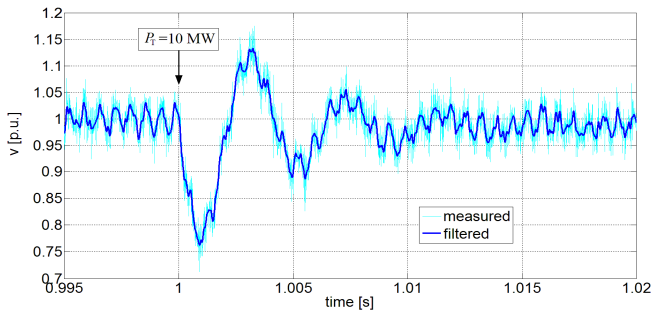

Figure 6. Bus voltage transient (Test 1, Scenario 1, P_T=10 MW in t=1 s).

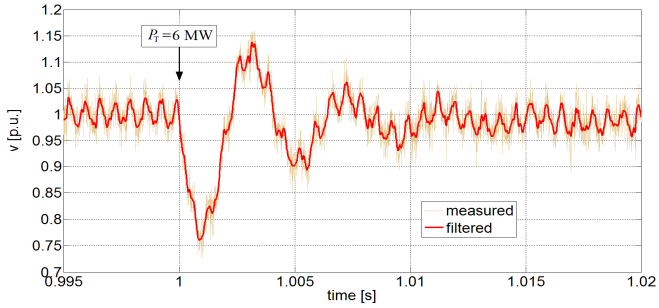

Figure 7. Bus voltage transient (Test 2, Scenario 2, P_T=6 MW in t=1 s).

The outcomes of the described procedure are expressed in Figs. 6-7, which show the signals of the two tests. In such figures, it is important to notice that start-up signals (cyan/grey sampled transients) are given by a multiconverter detailed switching model, originating from the one successfully used in [9] and validated by RTDS detailed model of [14]. Although the start-up transients are indeed not resulting from a test campaign on a real MVDC shipboard power system, the signal nature does not invalidate the proposed procedure for estimating system parameters, whose potentiality will be demonstrated in section V.

B. Reduced Model for Estimation

By starting from the model of Fig. 4 and considering the operating conditions as specified during tests (F=0, linear power P_T), the reduced model for the estimation procedure (using e as a superscript) is given by Fig. 8, where $R_T=P_T/V_0^2$.

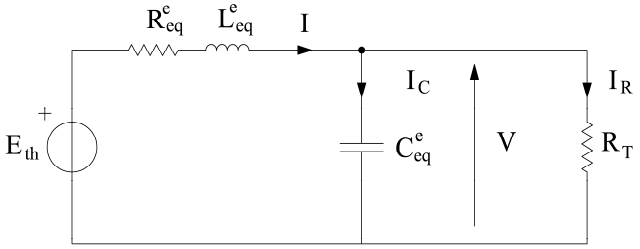

Figure 8. Reduced model for estimation.

When studying such a circuit, the voltage dynamics are easily determined by equation (20). This equation can be rearranged as differential equation (21), to be employed in the estimation, by substituting the ratio L_{eq}^e/R_{eq}^e with the time constant T_f^e.

$$\ddot{V}+\left(\frac{R^e_{eq}}{L^e_{eq}}+\frac{1}{C^e_{eq}R_T}\right)\cdot\dot{V}+\left(\frac{1}{L^e_{eq}C^e_{eq}}+\frac{R^e_{eq}}{L^e_{eq}C^e_{eq}R_T}\right)\cdot V=\frac{E_{th}}{L^e_{eq}C^e_{eq}} \quad (20)$$

$$\ddot{V}+\left(\frac{1}{T^e_f}+\frac{1}{C^e_{eq}R_T}\right)\cdot\dot{V}+\left(\frac{1}{L^e_{eq}C^e_{eq}}+\frac{1}{T^e_fC^e_{eq}R_T}\right)\cdot V=\frac{E_{th}}{L^e_{eq}C^e_{eq}} \quad (21)$$

C. Methods for Parameter Estimation

The proposed method seeks to produce a low dimensional system, whose model parameters ($T_f{}^e$, L_{eq}^e, C_{eq}^e) are conveniently tuned to obtain a very close correspondence among the resulting voltage transient (21) and the filtered bus voltage transient based on (simulated) measurements as shown in Figs. 6-7. In the presence of a good convergence among simulated (21) and measured transients (small RMSE), the model parameters computed in the last iteration are able to approximate the unknown parameters ($T_f{}^*$, L_{eq}^*, C_{eq}^*), thus making possible the determination of a suitable linearizing function F. Therefore, the estimation procedure is delineated as a nonlinear multi-objective optimization problem, the input voltage transients being nonlinear. However, the computational complexity in solving this nonlinear problem by means of linear or dynamic programing techniques motivates us to exploit other possibilities for obtaining the parameters. In this context, heuristic approaches appear as a good alternative, thus two methods, one deterministic and one stochastic, are proposed:

- a simplified version of the exhaustive search method, dubbed Selective Search (SS), able to confine the search-space to an acceptable range (subsection IV-D);
- a Particle Swarm Optimization (PSO) in order to validate the proposed SS method (subsection IV-E).

D. Selective Search procedure (SS)

The general idea of the SS procedure follows the exhaustive search procedure, but instead of trying all possible solutions, the search is only concentrated around the optimum value (true parameters) in equidistantly spaced intervals (22):

$$T_f^e \in [0.7T_f, 1.3T_f] \quad L_{eq}^e \in [0.7L_{eq}, 1.3L_{eq}] \quad C_{eq}^e \in [0.7C_{eq}, 1.3C_{eq}] \quad (22)$$

As a matter of fact, the true equivalent parameters (T_f^*, L_{eq}^*, C_{eq}^*) are expected to be in the vicinity (±30%) of the designed values (T_f, L_{eq}, C_{eq}), therefore the assumption (22) is verified and able to properly confine the parameters' domain. Thus, an equal number of candidate solutions, $\alpha \in N$, are generated in every interval. A smoothed interpolation through this cloud of points can subsequently be created to see the relationship between these residuals and the real power system data. The corresponding error will reflect the linear and non-linear components. Therefore, the computational complexity is reduced from $O(n^3)$ in the case of exhaustive search procedure to $O(\alpha^3)$. The search space is explored in Matlab® until 1000 points, thus $f_\alpha(T_f^e, L_{eq}^e, C_{eq}^e) : R^3 \rightarrow R, \forall\, \alpha \in N$ with $\alpha=\{2\ldots10\}$.

E. Particle Swarm Optimization (PSO)

Introduced by Russell Eberhart and James Kennedy in 1995, Particle Swarm Optimization (PSO) [16] is one of the most popular heuristic stochastic algorithms able to find a solution to complex non-linear optimization problems by imitating the behavior of bird flocks. In the cases studied in this paper, the speed of the swarm is set equal to 10^{-5}, whereas the cognitive parameter is c_1=1 and the social parameter is put equal to c_2=4-c_1. To improve the estimation in terms of computation time versus accuracy, the choice of the swarm size (number of particles) and the optimal number of iterations is carefully investigated in the next subsections.
The performance of this method has been mentioned in several studies, e.g. [25]. Besides that, based on our previous work [26], in which we performed a comparison between Minimax algorithm, genetic algorithms, PSO, and quantum particle swarm optimization to optimally allocate the energy resources in buildings, the choice of PSO seemed naturally suited.

F. Estimation Results

The two proposed methods (SS and PSO) are employed for estimating the system parameters in the two scenarios of interest, i.e. Scenario 1 and Scenario 2. To assess the accuracy of SS and PSO, two metrics are used: the RMSE between the filtered signal and the voltage model output, and the computational time requirements T. For each scenario, the metrics will be compared to establish the best method.

Figures 9-10 illustrate the ability of the proposed estimation methods to capture the voltage transients, where the convergence between the input filtered signals (cyan curves) and the reduced model transients is increasing as the number

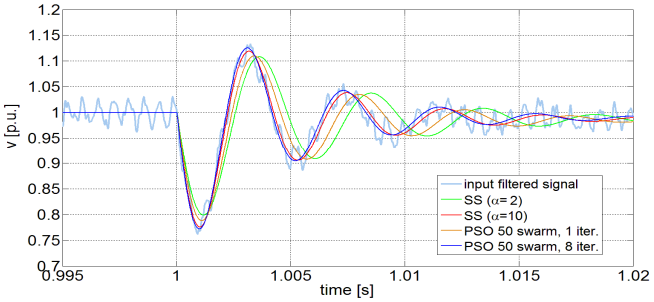

Figure 9. Estimation procedure (Scenario 1).

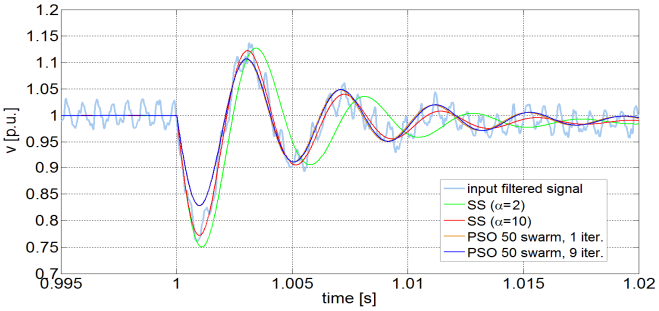

Figure 10. Estimation procedure (Scenario 2).

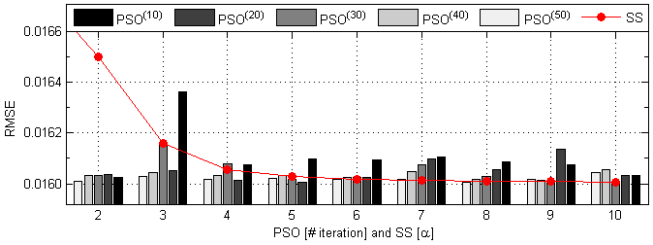

Figure 11. RMSE values for Scenario 1 using SS and PSO.

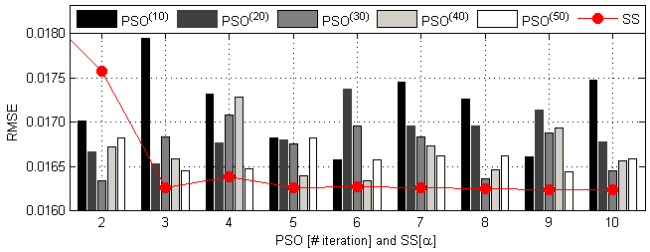

Figure 12. RMSE values for Scenario 2 using SS and PSO.

of iterations grows. In particular, for both scenarios the best correspondence (smallest RMSE) is guaranteed by 10 iterations of SS, whereas the best PSO method (with 50 swarm particles) performs less accurately. The best correspondence with the reference signals is obtained after 10 iterations for SS and after 8 (Scenario 1) or 9 (Scenario 2) iterations for the PSO, after which the RMSE remains almost constant. In this regard, the evolution of the RMSE values for Scenario 1 is depicted in Fig. 11. Particularly, although the final results for Scenario 1 (Fig. 9) are shown for 50 swarm particles, the PSO parameter estimation has been investigated using various numbers of particles (10, 20, 30, 40) as observable in Fig. 11. Similar considerations may be made also for Scenario 2. For the two scenarios, the estimation results are reported in Table V, where the data reported on rows labeled SS_{10} are related to

TABLE V. Estimation results, Scenario 1 and Scenario 2

		T_f^e [ms]	L_{eq}^e [mH]	C_{eq}^e [µF]	R_{eq}^e [mΩ]	RMSE	PCC	T [s]
SCENARIO 1	DESIGN	13.79	0.65	923.61	47.49	0.0180	0.04	2
	SS_2	9.65	0.46	1200.69	47.49	0.0172	0.13	11
	SS_{10}	14.24	0.63	708.10	44.42	0.0160	0.90	1417
	PSO_1	12.56	0.56	815.54	44.75	0.0161	0.93	115
	PSO_8	14.73	0.64	703.12	43.60	0.0160	0.99	541
SCENARIO 2	DESIGN	13.79	1.05	577.26	75.98	0.0183	0.03	3
	SS_2	17.92	1.36	404.08	75.98	0.0176	0.05	11
	SS_{10}	15.17	1.08	404.08	71.37	0.0162	0.90	1402
	PSO_1	14.79	0.76	549.93	51.15	0.0165	0.95	119
	PSO_9	15.26	0.76	556.73	49.64	0.0164	0.99	579

TABLE VI. Estimated filters parameters, using SS_{10}.

	SCENARIO 1			SCENARIO 2	
	BF1	BF2	BF3	BF1	BF2
R_{fk}^e [mΩ]	118.46	177.69	118.46	118.96	178.44
L_{fk}^e [mH]	1.69	2.53	1.69	1.80	2.71
C_{fk}^e [µF]	265.54	177.02	265.54	242.45	161.63

TABLE VII. Installed filter parameters versus control parameters.

	BF1	BF2	BF3
R_{fk}^* [mΩ]	105.10	224.14	111.44
R_{fk}^c [mΩ]	118.71	178.06	118.46
L_{fk}^* [mH]	1.80	2.44	1.68
L_{fk}^c [mH]	1.75	2.62	1.69
C_{fk}^* [µF]	245.91	173.18	273.62
C_{fk}^c [µF]	254.00	169.33	265.54

the best estimation, with the smallest RMSE (although largest execution time). Due to the small RMSE values obtained with both methods, to be able to choose the most suitable one, we used the Pearson correlation coefficient (PCC) to understand better the relation between the real and the predicted values. PCC takes values between -1 and 1. Very small PCC values, close to zero (like in the Design phase), show that there is not any relation between the estimated and the real values, while PCC values close to 1 reflect a perfect correlation. Overall, the proposed Selective Search method shows better accuracy levels in terms of RMSE in comparison with PSO for the estimation procedure solved here, and somewhat smaller PCC values. This is given by the fact that at every iteration PSO checks more solutions than SS. This small benefit of PSO is down sided by its lower stability in convergence behavior in comparison with SS.

Since the estimation is capable of only offering the equivalent parameters, the actual filter parameters are to be approximated. Particularly, by hypothesizing that the ratio among single estimated parameter (X^e) and equivalent estimated parameter (X_{eq}^e) is equal to the ratio between single designed parameter (X) and equivalent designed parameter (X_{eq}), the values of Table VI may be easily calculated. Finally, the values in Table VII are set for each DC-DC converter controller by taking the average between the estimated values in the two scenarios. It is worthy of note how the performed procedure offers an accurate estimation of the installed parameters, with special regard to the most critical capacitive terms. Indeed, by calculating the equivalent estimated capacitance in the two scenarios, the resulting K term (C_{eq}^*/C_{eq}^c) is practically equal to 1, revealing how the combination of LSF and SS estimation procedure can ensure the bus voltage stability.

V. PERFORMANCE OF THE PARAMETER ESTIMATION

The procedure described so far is based on the two off-line tests detailed in subsection IV-A. Such tests provide the input transients for the SS method, aimed at estimating the control parameters reported in Table VII. To verify the reliability of the proposed methodology, and thus the actual capability of calibrating a proper linearizing function, some simulations are performed in subsections V-B and V-C for assessing the bus voltage stability. Since the power system topology shown in Fig. 1 is identical to what was studied in [14], also the centralized strategy for controlling the bus voltage as described in subsection V-A is equal to that described in [14].

A. Bus Voltage Control

As envisaged in [14], the bus voltage is regulated by the combined action of DC-DC converters, whose output voltages are forced by duty cycle commands. The latter are given by the algebraic sum of signals originating from different controllers: a decoupled outer (slow) integral controller to reach the operating point V_0, and internal (fast) LSF controllers to compensate for the CPL and to guarantee the desired voltage dynamics. Considering the double functionality required for an internal controller (nonlinear stability and linear dynamics), also double is the output: a linearizing function f_l obtained by splitting the function F among the on-line converters, and a control function f_c to achieve the pole-placement for the resulting (presumably) linear system [14].

B. Simulations

By implementing the voltage control strategy in the manner explained in [14], some simulations may be carried out in a Matlab-Simulink environment to validate the parameter estimation. As a matter of fact, the Average Value Model (AVM) constitutes a valuable choice for testing the control, being already verified with real-time detailed model implementation in RTDS [14]. To evaluate the benefits of the estimation procedure, the multiconverter power system is configured by installed parameters (X_{fk}^*), while the control parameters for setting the linearizing function f_l are selected differently. Particularly, they are put equal to X_{fk}^* (Table VII), or to the designed parameters X_{fk} (Table II) or to the estimated ones X_{fk}^c (Table VII): this choice allows us to value the effect of parameter estimation on the bus voltage dynamics. Also the function f_c is conceived for ensuring two different control specifications (ξ damping factor and ω_0 natural frequency of the presumably linear system given by the LSF action): f_{c1} is determined for ensuring the behavior seen in [14] (ξ=0.3, ω_0=1500 rad/s), while f_{c2} offers somewhat worse performance characterized by ξ=0.16 and ω_0=1200 rad/s.

C. Results

For studying the bus voltage dynamics in a critical case, the LSF controlled power system is perturbed by the loss of the

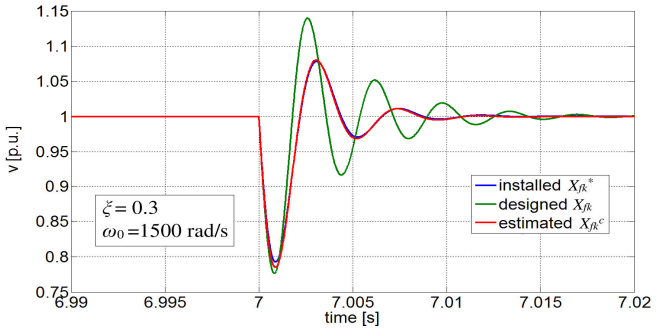

Figure 13. Bus voltage transient (p.u., linearization f_l, pole-placement f_{c1}).

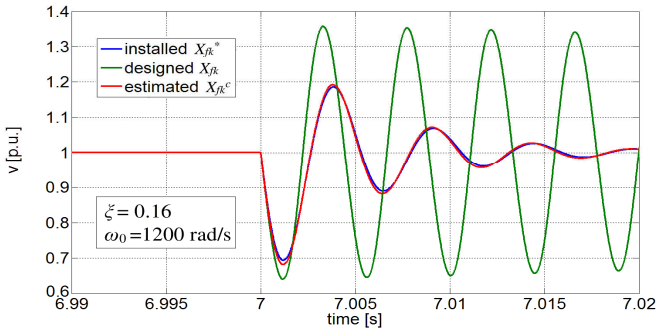

Figure 14. Bus voltage transient (p.u., linearization f_l, pole-placement f_{c2}).

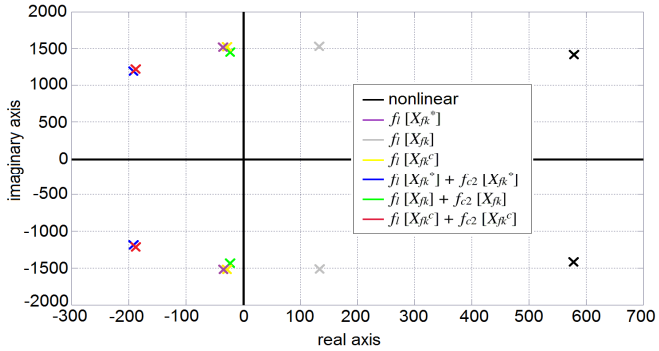

Figure 15. Root-locus by applying f_l and f_{c2}.

DC-DC buck converter B3 at t=7 s. This eventuality is simulated by the instantaneous opening of CB_3. In particular, Fig. 13 shows the bus voltage transients, when linearizing function f_l and control f_{c1} are activated, whereas the control function is changed to f_{c2} for the results in Fig. 14. By observing Fig. 13, the correspondence among the blue and red transients (installed parameters versus estimated parameters) is remarkable. This suggests the potentiality of the performed estimation, whose parameters are able to correctly emulate the behavior of a perfectly linearized system (blue curve). This means that a linearizing function based on X_{fk}^c parameters is capable of making the system linear. Different conclusions can be drawn for the transient given by the designed parameters (green curve), whose dissimilarity with the blue curve signifies that only a partial linearization can be achieved when X_{fk} are used. If the partial linearization of Fig. 13 is not a critical issue, but rather a performance worsening compared to the control specifications, by contrast the green transient of Fig. 14 reveals a perilous scenario, characterized by an underdamped behavior (v_{max}=1.36, v_{min}=0.64) and a tenfold increase in settling time (about 0.2 s). The latter is also confirmed in the root-locus shown in Fig. 15, obtained by linearizing equation (8) in the equilibrium point (V_0, I_0) and adding a proportional-derivative (PD) control function f_{c2} for the pole-placement. Particularly, a partial linearization based on X_{fk} parameters is incapable of moving the poles from the initially unstable position (black) to a stable position in the left half-plane. From the resulting unstable poles (grey), the effect of the control function f_{c2} moves the poles left, close to the imaginary axis, however it is insufficient (green poles, ξ=0.015 and ω_0=1450 rad/s) in providing the expected control specifications. Conversely, for a linearization based on X_{fk}^c, the location of the yellow poles already denotes system stability. Thus, the function f_{c2} can effectively place the final complex poles (red) in a position very close to the expected ones (blue, ξ=0.16 and ω_0=1200 rad/s).

VI. Conclusions

The Linearization via State Feedback (LSF) is recognized as a valuable strategy for solving the CPL instability in multiconverter MVDC shipboard power systems. Nevertheless, this technique is able to linearize the nonlinear loads only when accurate knowledge of the filter parameters is available. Conversely, in the presence of a parameter mismatch between the installed parameters and those used for the controllers setting, only a partial, or even insufficient, linearization is achievable. To solve this issue, the paper has proposed an estimation procedure for determining the filter parameters. Particularly, such a procedure is based on off-line tests for providing the reference voltage transients. The latter has constituted the input data for two estimation methods (Selective Search and Particle Swarm Optimization), to establish the control parameters necessary for tuning the LSF controllers, thus guaranteeing a resulting linear system on which to apply the desired pole-placement. The effectiveness of the estimation procedure has been evaluated by dynamic simulations, which highlight how a LSF control tuned purely on designed parameters is incapable of completely linearizing the system. Although the system stability may be ensured by the control function, the root-locus has shown a clear worsening in control performance in the case presented. In general, since the initial positions of the unstable poles are unknown, and neither are the consequent positions after the application of the linearizing function, the control function could be insufficient for stabilizing a system whose control is based on designed parameters. For such a reason, the parameter estimation is paramount, and actually not limited to the power system stability problem. Indeed, since the short-circuit current in the DC circuit is strongly dependent on the capacitor components, the estimation can be very useful for correctly setting the DC circuit-breaking devices as well.

Acknowledgment

Authors wish to thank Prof. Giovanni Giadrossi and Prof. Fabrizio Russo of the Department of Engineering and Architecture, University of Trieste, for valuable contributions given to the realization of this work.

REFERENCES

[1] Fei Wang, Zheyu Zhang, T. Ericsen, R. Raju, R. Burgos and D. Boroyevich, "Advances in Power Conversion and Drives for Shipboard Systems", *Proceedings of the IEEE*, vol. 103, no. 12, pp. 2285–2311, Dec. 2015.

[2] A. Vicenzutti, D. Bosich, G. Giadrossi, G. Sulligoi, "The Role of Voltage Controls in Modern All-Electric Ships: Toward the all electric ship", *IEEE Electrification Magazine*, vol. 3, no. 2, June 2015.

[3] G. Sulligoi, A. Vicenzutti, V. Arcidiacono, Y. Khersonsky, "Voltage stability in large marine integrated electrical and electronic power systems", *IEEE Transactions on Industry Applications*, vol. 52, no. 4, pp. 3584 - 3594, March 2016.

[4] IEEE Std. 1709-2010, "IEEE recommended practice for 1 to 35kV medium voltage DC power systems on ships", *DC Power Systems on Ships Working Group of the IEEE Industry Applications Society Petroleum & Chemical Industry (IAS/PCI) Committee*, 2010.

[5] J. Kuseian, T.J. McCoy and K.M. McCoy, "Naval Power Systems Technology Development Roadmap PMS 320", *Naval Sea Systems Command*, 2013.

[6] S. D. Sudhoff, "Currents of Change", *IEEE Power and Energy Magazine*, vol. 9, no. 4, pp. 30-37, July-August 2011.

[7] D. Bosich, A. Vicenzutti, R. Pelaschiar, R. Menis and G. Sulligoi, "Toward the Future: the MVDC Large Ship Research Program", *Proc. AEIT Annual Conference 2015*, Oct. 14–16, 2015, Napoli, Italy.

[8] A. Kwasinski and C. N. Onwuchekwa, "Dynamic behavior and stabilization of DC microgrids with instantaneous constant-power loads", *IEEE Trans. Power Electron.*, vol. 26, no. 3, pp. 822–834, Mar. 2011.

[9] V. Arcidiacono, A. Monti and G. Sulligoi, "Generation control system for improving design and stability of medium-voltage DC power systems on ships", *IET Electrical Systems in Transportation*, vol. 2, no. 3, pp. 158–167, Sep. 2012.

[10] M. Cupelli et al., "Power Flow Control and Network Stability in an All-Electric Ship," *Proceedings of the IEEE*, vol. 103, no. 12, pp. 2355-2380, Dec. 2015.

[11] A. M. Rahimi and A. Emadi, "Active damping in DC/DC power electronic converters: a novel method to overcome the problems of constant power loads", *IEEE Trans. Ind. Electron.*, vol. 56, no. 5, pp. 1428–1439, May 2009.

[12] G. Sulligoi, D. Bosich, V. Arcidiacono and G. Giadrossi, "Considerations on the design of voltage control for multi-machine MVDC power systems on large ships",*Proc. IEEE Electric Ship Technologies Symposium (ESTS) 2013*, pp. 314–319, Apr. 22-24, 2013, Arlington (VA), USA.

[13] A. M. Rahimi, G. A. Williamson, and A. Emadi, "Loop cancellation technique: a novel nonlinear feedback to overcome the destabilizing effect of constant-power loads," *IEEE Trans. Vehic. Technol.*, vol. 59, no. 2, pp. 650–661, Feb. 2010.

[14] G. Sulligoi, D. Bosich, G. Giadrossi, L. Zhu, M. Cupelli and A. Monti, "Multi-Converter Medium Voltage DC Power Systems on Ships: Constant-Power Loads Instability Solution using Linearization via State Feedback Control", *IEEE Transactions on Smart Grid*, vol. 5, no. 5, Sept. 2014.

[15] G. Sulligoi, D. Bosich, and G. Giadrossi, "Linearizing voltage control of MVDC power systems feeding constant power loads: stability analysis under saturation," *Proc. IEEE Power and Energy Soc. (PES) General Meeting*, Vancouver, BC, Canada, Jul. 21–25, 2013, pp. 1–5.

[16] J. Kennedy and R. Eberhart, "Particle swarm optimization," *Proc. IEEE International Conference on Neural Networks*, Perth, WA, 1995, pp. 1942-1948 vol.4.

[17] M. Cupelli, L. Zhu and A. Monti, "Why Ideal Constant Power Loads Are Not the Worst Case Condition From a Control Standpoint," *IEEE Transactions on Smart Grid*, vol. 6, no. 6, pp. 2596-2606, Nov. 2015.

[18] MAIB safety bulletin 4/2010, "Catastrophic failure of a capacitor and explosion in an 11kV harmonic filter on board the passenger cruise vessel RMS Queen Mary 2", *online*.

[19] A. Berizzi, A. Silvestri, D. Zaninelli and S. Massucco, "Short-circuit current calculations for DC systems", *IEEE Transactions on Industry Applications*, vol. 32, no. 5, pp. 990-997, Sep/Oct 1996.

[20] A. M. R. Amaral and A. J. M. Cardoso, "On-line fault detection of aluminium electrolytic capacitors, in step-down DC-DC converters, using input current and output voltage ripple", *IET Power Electronics*, vol. 5, no. 3, pp. 315–322, March 2012.

[21] H. K. Khalil, Nonlinear systems. New York, USA, Macmillan, 1992.

[22] D. Bosich, G. Giadrossi, G. Sulligoi, S. Grillo and E. Tironi, "More Electric Vehicles DC Power Systems: a Large Signal Stability Analysis in presence of CPLs fed by Floating Supply Voltage", *Proc. IEEE IEVC 2014*, pp. 1–6, Dec. 17-19, 2014, Florence, Italy.

[23] C. Tomasi, R. Manduchi, "Bilateral filtering for gray and color images", *Proc. IEEE International Conference on Computer Vision*, Bombay, India, Jan. 4-7, 1998.

[24] F. Russo, F. Travain, "Rapid Prototyping of DSP Code for PC-Based Multi-Function Oscilloscopes", *International Journal of Circuits, Systems and Signal Processing*, Vol. 10, 2016.

[25] M. R. AlRashidi, M. F. AlHajri, A. K. Al-Othman and K. M. El-Naggar, "Particle Swarm Optimization and Its Applications in Power Systems", *Computational Intelligence in Power Engineering*, 2010, pp. 295-324.

[26] S. Markidis, E. Mocanu, M. Gibescu, , P.H. Nguyen and W.L. Kling, "Benchmarking algorithms for resource allocation in smart buildings", *Proc. IEEE PowerTech 2015*, June 29-July 2, 2015, Eindhoven, The Netherlands.

Daniele Bosich (M'07) received the M.S. degree (with honors) in electrical engineering from the University of Trieste, Italy, in 2010, and the Ph.D. degree in energy engineering at the University of Padua, Italy, in 2014. Dr. Bosich is the author of more than 20 scientific papers in the fields of marine shipboard power systems and voltage control. He is a member of PES and IAS.

Giorgio Sulligoi (M'02) received the M.S. degree (with honors) in electrical engineering from the University of Trieste, Italy, in 2001, and the Ph.D. degree in electrical engineering from the University of Padua, Italy, in 2005. He spent an internship at Fincantieri Electric Systems Office (Trieste), and a semester as a Visiting Scholar at the University College of Cork (Ireland). In 2005, he joined MAI Control Systems, Milan, Italy, an Italian firm operating in the field of power stations and alternator voltage control systems. Since 2007 he is an Assistant Professor of electric power generation and control in the Department of Engineering and Architecture, University of Trieste (Italy). He is member of PES, where he serves in the MARSYS committee.

Elena Mocanu received the B.Sc. degree in Mathematics and Physics from Transilvania University of Brasov, Romania, the M.Sc. degree in Physics from University of Bucharest, Romania, in 2011 and the M.Sc. degree in Operational Research from Maastricht University, The Netherlands, in 2013. She has been a Assistant Lecturer within the Department of Information Technology, University of Bucharest, Romania from September 2008 to January 2011. She is currently a Ph.D. student in the Department of Electrical Engineering, Eindhoven University of Technology, The Netherlands.

Madeleine Gibescu received her Dipl.Eng. in Power Engineering from the University Politehnica, Bucharest, Romania in 1993 and her MSc and Ph.D. degrees in Electrical Engineering from the University of Washington, Seattle, WA, U.S. in 1995 and 2003, respectively. She has worked as a Research Engineer for ClearSight Systems, and as a Power Systems Engineer for Alstom Grid, in Washington and California, U.S. From 2007, she has worked as an Assistant Professor for the Electrical Sustainable Energy Department, Delft University of Technology, the Netherlands. Currently she is an Associate Professor with the Electrical Energy Systems Department, Eindhoven University of Technology, the Netherlands. Her research interests are in the area of smart and sustainable power systems.